Hindawi Publishing Corporation
Advances in Materials Science and Engineering
Volume 2016, Article ID 8205984, 7 pages
http://dx.doi.org/10.1155/2016/8205984

Research Article

Preparation of *Antheraea pernyi* Silk Fibroin Microparticles through a Facile Electrospinning Method

Xiufang Li,[1,2] Qiang Zhang,[1] Yanfei Feng,[1] Shuqin Yan,[1] Jing Qu,[2] and Renchuan You[1]

[1]*College of Textile Science and Engineering, Wuhan Textile University, Wuhan 430200, China*
[2]*National Engineering Laboratory for Modern Silk, College of Textile and Clothing Engineering, Soochow University, Suzhou 215123, China*

Correspondence should be addressed to Renchuan You; yourenchuan1182@126.com

Received 16 April 2016; Revised 9 July 2016; Accepted 20 July 2016

Academic Editor: Mikhael Bechelany

The goal of this study was to fabricate *Antheraea pernyi* silk fibroin (ASF) microparticles using electrospinning under mild processing conditions. To improve processability of the ASF solution, poly(ethylene oxide) (PEO) was used to regulate viscosity of ASF solution for electrospinning. It was found that the blend of ASF with PEO could form a bead-on-string structure with well spherical particles. Furthermore, aqueous ethanol and ultrasonic treatments could disrupt the nanofibrillar string structure between particles and ultimately produced water-insoluble ASF particles with submicron scale. Cell viability studies indicated that the ASF microparticles were nontoxic to EA926 cells. Moreover, fluorescent images based on FITC labeling showed that the ASF microparticles were easily uptaken by the cells. Aqueous-based electrospinning provides a potentially useful option for the fabrication of ASF microparticles based on this unique fibrous protein.

1. Introduction

Silk fibroin (SF) is an appealing material for numerous biomedical applications involving drug delivery, tissue engineering, or implantable devices because of its abundance, biocompatibility, and biodegradability [1–3]. The silk fibers can be dissolved in aqueous systems, followed by reprocessing into desired material formats, such as films, fibers, and particles. Although water-in-oil emulsion, salting-out, self-assembly, and spray-drying have been successfully used to prepare SF-based particles [4–9], a challenge remains to prepare micro/nanoparticles that possess better bioactivity and avoid using organic solvents, concentrated salts, or other harsh processing for achieving improved biocompatibility.

Silks can be classified as mulberry and nonmulberry. *Antheraea pernyi* silk is the most extensively applied nonmulberry silk in industry. Increasing evidences show that *Antheraea pernyi* SF (ASF) exhibited better bioactivity than mulberry SF due to the presence of integrin adhesion receptor Arg-Gly-Asp (RGD) tripeptide [9–13]. ASF particles should have higher cellular targeting ability through specific RGD-integrin interactions. Therefore, developing a simple and green method for the fabrication of ASF microparticles from aqueous system will be attractive.

Electrospinning is a versatile approach to fabricate micro/nanofibers. The regulation in electrospun parameters is able to form a bead-on-string structure or even particles instead of fibers [14]. Thus, the fabrication of SF particles by adjusting electrospun parameters is assumed to be possible. The aqueous-based electrospinning would provide a green method to prepare ASF particles without organic solvents such as hexafluoroisopropanol (HFIP) and formic acid. However, the regulation ability of morphology for electrospinning from only aqueous SF solution is limited due to its insufficient viscosity [15, 16]. Herein, we developed a facile and green electrospinning method to produce ASF microparticles by using biocompatible polymer poly(ethylene oxide) (PEO) to regulate ASF solution viscosity. The bead-on-string structure formed after blending with PEO and the string structure between beads could be disrupted to obtain dispersive ASF microparticles after aqueous ethanol and ultrasonic treatment.

Table 1: Blend ratios, concentrations, and viscosity of electrospinning solutions.

Sample number	ASF ((w/v)%)	PEO ((w/v)%)	Solution viscosity (mPa·S)
1	16.0%	0	46.4 ± 7.5
2	24.0%	0	70.5 ± 15.2
3	0	0.8%	40.6 ± 10.1
4	0	3.2%	181.4 ± 4.6
5	0	5.0%	928.1 ± 27.1
6	16.0%	0.8%	168.4 ± 42.2

2. Materials and Methods

2.1. Preparation of Regenerated ASF Solution. Regenerated ASF solution was prepared following the procedure described previously [10]. In brief, *Antheraea pernyi* raw silks (Dandong, Liaoning, China) were boiled three times in a 0.25% Na_2CO_3 solution for 30 min. The extracted fibroin was dissolved in molten $Ca(NO_3)_2$ at 100°C ± 2°C for 4 h and then dialyzed (MWCO 9–14 kDa) in deionized water for 3 days. The ASF solution was lyophilized and then redissolved in deionized water for various concentrations.

2.2. Electrospinning. A 5.0% PEO solution (average MW 300,000, Aldrich) was added into ASF solution to form blends. The concentration and blend ratio are as shown in Table 1. The solution viscosity was measured using a rotational rheometer (AR 2000, TA Instruments) at 25°C. The electrospinning was performed at a flow rate of 1 mL/h under 15 kV voltage field, and the distance between needle tip and grounded target was 15 cm. The electrospun products were deposited on the aluminum foil.

2.3. Preparation of ASF Microparticles. The electrospun beaded nanofibers were immersed in 90% aqueous ethanol and then treated by using an ultrasonic cell disruptor with an energy output of 300 W for 60 times (10 s for each time). A certain amount of ultrapure water was added into particle suspension to form 75% ethanol aqueous solution, and the ASF particles were immersed in 75% ethanol for 1 h to make the particles water-insoluble and sterile. The dispersive particles were shook at 100 rpm for 24 h to remove PEO [17, 18]. The suspensions were centrifuged at 13,000 rpm for 10 min, and the pellets were washed twice and resuspended in sterilized ultrapure water. The resulted ASF microparticle suspensions were lyophilized using a freezing dryer.

2.4. Characteristics of ASF Microparticles. Dynamic light scattering (DLS) was performed to measure the size of ASF particles with Zetasizer (Nano ZS, Malvern, Worcestershire). One milliliter of ASF particle suspension was used in disposable polystyrene cuvettes with a 10 mm path length. The data were recorded at 25°C. The sample morphologies were observed by a scanning electron microscope (SEM; Hitachi S-4800, Japan). A 100 μL of ASF particle suspension was directly added on top of a conductive tape mounted on a sample stub. The samples were dried overnight in air and then observed using SEM after gold sputtering. To investigate the conformation of ASF particles, the lyophilized particles were prepared in KBr pelleting for FTIR spectra analysis. Fourier transformed infrared spectroscopy (FTIR) data were recorded with a Nicolet 5700-spectrometer (Thermo Fisher Scientific).

2.5. FITC Labeling of Microparticles. ASF microparticles were labeled with fluorescein isothiocyanate (FITC; Sigma-Aldrich). 300 μL of FITC solution (10 mg/ml in dimethyl sulfoxide) was added to 10 ml of 1 mg/ml ASF microparticle suspension in bicarbonate buffer (pH = 8.5, 0.1 M). The reaction was allowed to proceed for 2 h in the dark at room temperature. Next, 200 μL of 1 M hydroxyl ammonium chloride solution was added and stirred for 10 min at room temperature. To remove the unreacted FITC, the microparticles were subjected to repeated cycles of washing and centrifugation (13,000 r/min for 10 min) until no fluorescence was detected in the supernatant (FM4P TCSPC fluorescence spectrophotometer, Horiba Jobin Yvon).

2.6. Culture of EA926 Endothelial Cells. EA926 cells (ATCC, USA) were cultured in Dulbecco's modified Eagle medium (DMEM, low glucose) supplemented with 10% fetal bovine serum (FBS) and 1% streptomycin-penicillin (Invitrogen, Carlsbad, CA, USA). Cell cultures were maintained in a humidified incubator at 37°C and 5% CO_2, and culture medium was replaced every 3 days.

2.7. Cellular Uptake and Cytotoxicity Test. EA926 cells were plated at a density of 2×10^4 cells/well in glass dishes for confocal microscopy observation. After 24 h of culture, the medium was replaced with fresh medium containing 500 μg/mL of FITC-labeled microparticles. After culture for 2 h, cellular uptake was observed by confocal microscopy. The cells were washed three times with phosphate buffer solution (PBS) and fixed in 4% paraformaldehyde in PBS for 30 min and then rinsed three times with PBS. The fixed cells were permeabilized with 0.2% Triton X-100 in PBS for 5 min and then blocked with 2% BSA in PBS for 30 min. The cell nuclei were stained with 5 μg/mL 4′,6-diamidino-2-phenylindole (DAPI, Sigma-Aldrich) for 10 min and rinsed thoroughly with PBS. The fluorescence images were obtained using a confocal laser scanning microscopy (CLSM; IX81/FV1000, Olympus, Japan). To determine the toxicity profile of the ASF microparticles, the cell viability was evaluated by CCK-8 assay. EA926 cells were plated at a density of 2×10^4 cells/well in 24-well plates. After 24 h of culture, the medium was

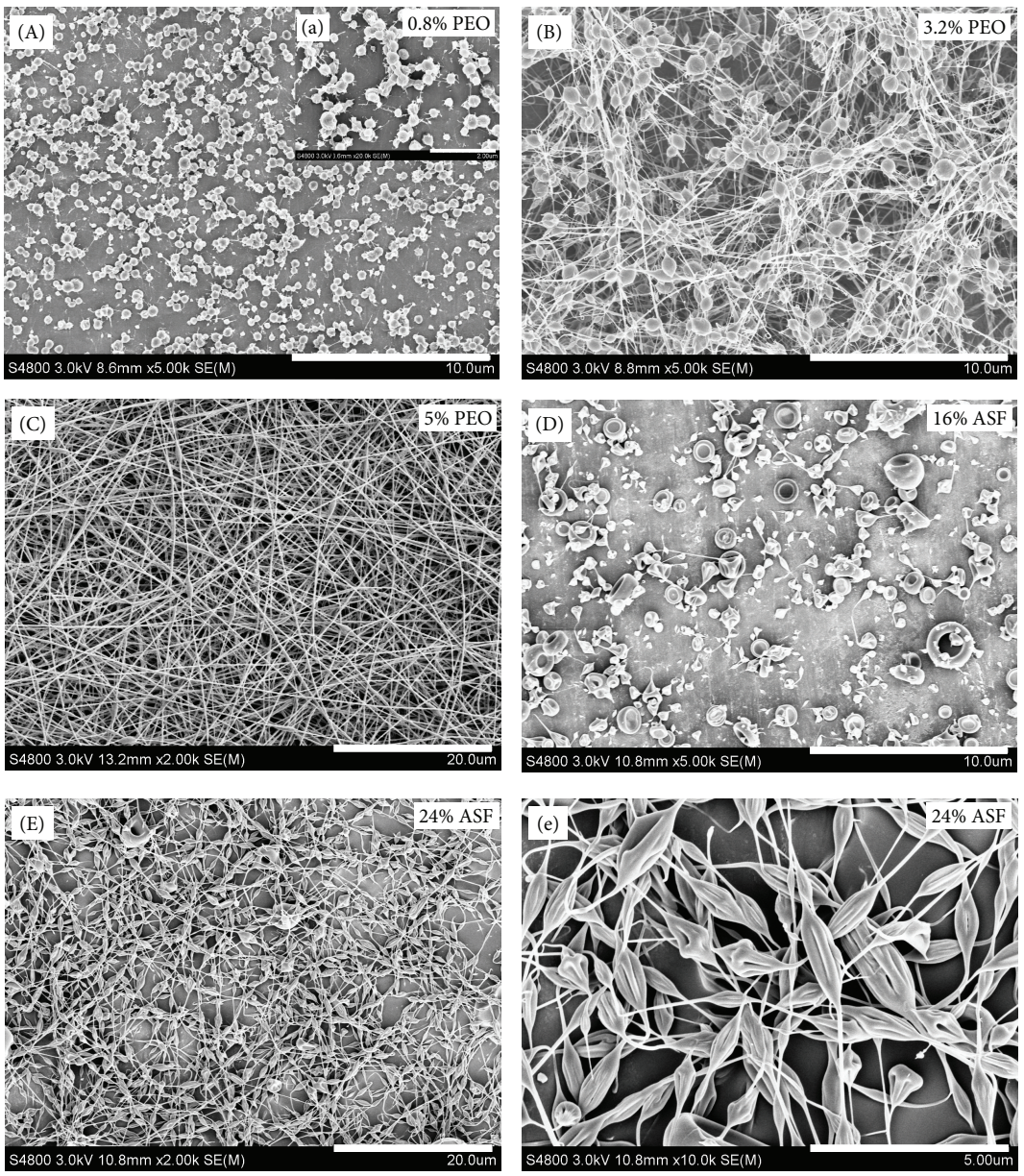

Figure 1: SEM images of electrospun products from various solutions: (A, a) 0.8 wt% PEO, (B) 3.2% PEO, (C) 5.0% PEO, (D) 16.0% ASF, (E) 24.0% ASF, and (e) magnified image of image (E). Scale bars: (A, B, D) 10 μm, (a) 2 μm, (C, E) 20 μm, and (e) 5 μm.

replaced with fresh medium containing ASF microparticles with varying concentrations. After 24 h, the growth medium was removed and 500 μL of fresh culture medium containing 50 μL of CCK-8 solution was added into each well and incubated in an incubator at 37°C and 5% CO_2 for 3 h. The absorbance of reaction medium from each well was measured at 450 nm using a microplate reader (Bio-Tek Synergy HT, USA). The wells without microparticles were used as the control.

3. Results and Discussion

Changing polymer concentration can control solution viscosity and then regulate the morphologies of electrospun products [19, 20]. PEO is well documented as a biocompatible polymer and has been applied to enhance *Bombyx mori* SF solution viscosity for preparing electrospun nanofibers [17, 18, 21]. When PEO concentration was changed from 0.8% to 3.2% and 5.0%, the corresponding viscosity was increased from 40.6 to 181.4 and 928.1 mPa·S (Table 1), respectively. Increasing viscosity resulted in obvious morphological changes from spherical particle to bead-on-string and nanofiber (Figures 1(A)–1(C)), indicating that PEO solution possesses remarkably good ability to regulate morphology for electrospun products, whereas only aqueous ASF solution is powerless. Numerous collapsed microparticles and undifferentiated drops from 16.0% ASF solution were electrosprayed on collector surface (Figure 1(D)) because the viscosity was

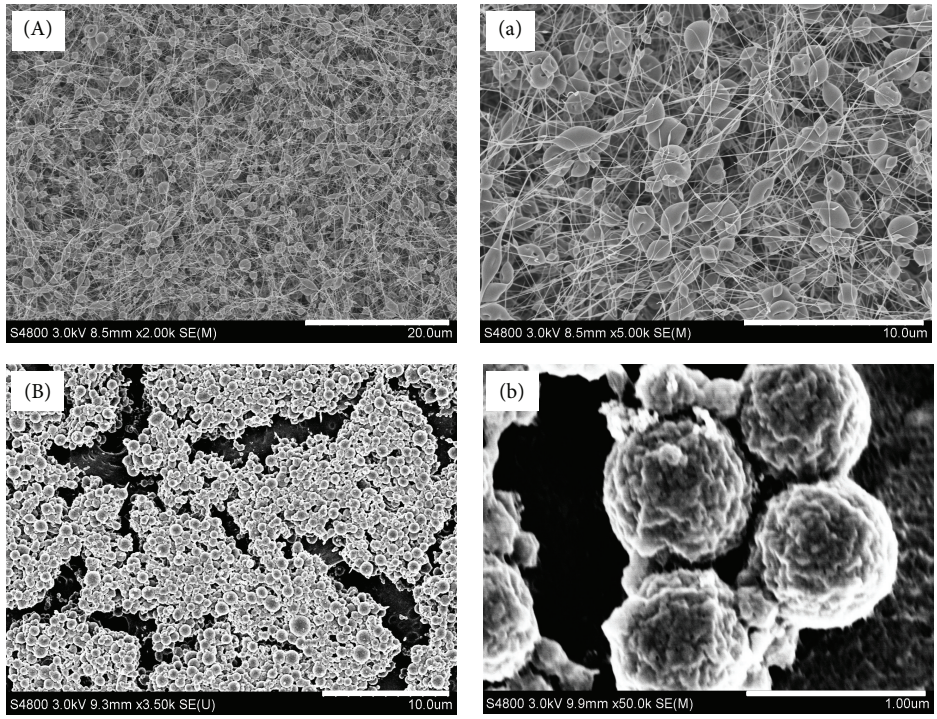

Figure 2: (A, a) SEM images of electrospun ASF/PEO bead-on-string structures and (B, b) SEM images of ASF particles. Scale bars: (A) 20 μm, (a, B) 10 μm, and (b) 1 μm.

not high enough to form stable jet. Increased viscosity can enhance chain entanglements to stabilize electrospinning jet [19, 20]. When ASF concentration was increased from 16.0% to 24.0%, the corresponding viscosity was increased from 46.4 to 70.5 mPa·S (Table 1) and led to the formation of bead-on-string morphology. However, the particles in bead-on-string showed a fusiform and collapsed morphology (Figures 1(E) and 1(e)).

After blending ASF with PEO (16.0% : 0.8%), the viscosity was increased to 168.4 mPa·s, which was approximate to the viscosity of 3.2% PEO solution. Increased viscosity led to the formation of bead-on-string structure with well spherical microparticles (Figures 2(A) and 2(a)). ASF can form water-insoluble β-sheet structure after aqueous ethanol treatment [22], whereas PEO is soluble in both water and ethanol. Therefore, the ASF/PEO nanofibrillar string (20–50 nm diameter) between particles could be readily disrupted after aqueous ethanol immersion and ultrasonic treatments (Figures 2(B) and 2(b)). SEM results showed that the obtained ASF particles had approximately 500–900 nm diameter (Figures 2(B) and 2(b)). DLS showed that the average diameter of ASF particles was about 801 ± 71 nm (Figure 3), which was consistent with SEM observation. The particles showed rough surface morphology and decreased diameters due to the extraction of PEO (Figure 2(b)).

The FTIR spectra were determined to investigate the structural change of ASF. The peaks at 1102 cm^{-1}, 962 cm^{-1}, and 840 cm^{-1} contribute to the characteristic peaks of PEO. After PEO addition into ASF, significant enhancement of peak intensity at 1102 cm^{-1} and 962 cm^{-1} was observed and

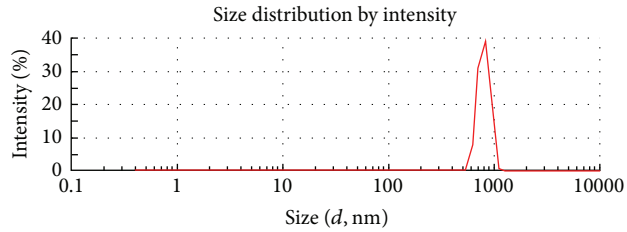

Figure 3: DLS size distribution of ASF particles.

a new peak at 840 cm^{-1} appeared (Figure 4). After ethanol treatment, the peaks at 1645 cm^{-1} (amide I, random coil) and 1545 cm^{-1} (amide II, random coil) shifted to 1629 cm^{-1} (amide I, β-sheet) and 1525 cm^{-1} (amide I, β-sheet), respectively, indicating that the structure of ASF changed to predominantly β-sheet (Figure 4). Moreover, the peak intensity at 1102 cm^{-1} and 962 cm^{-1} significantly decreased, and the peak at 840 cm^{-1} disappeared (Figure 4), demonstrating that the water soluble PEO had been extracted.

The submicron size of particles provides a number of distinct advantages for drug delivery system because they have relatively higher intracellular uptake and the ability to cross the physiological drug barriers [23]. Moreover, increasing evidences have demonstrated that RGD modification of microparticles enhanced targeting ability through RGD-integrin interaction [24]. ASF contains inherent RGD tripeptide sequences [10–12]. Therefore, ASF microparticles will be able to enhance cellular targeting ability through specific

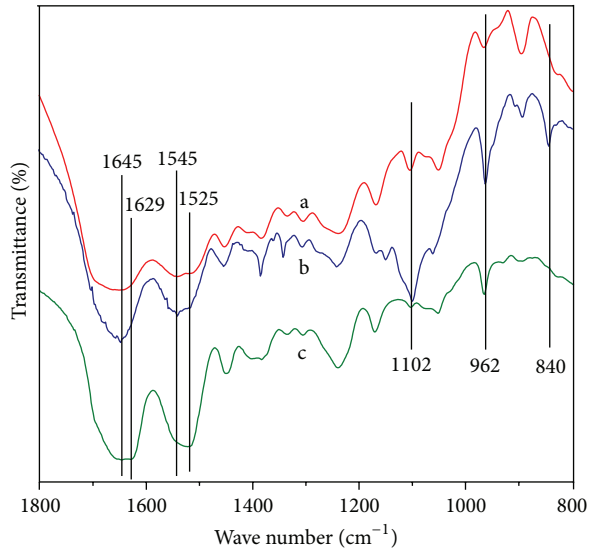

(a) Lyophilized ASF
(b) Electrospun ASF/PEO blend
(c) ASF nanoparticles

Figure 4: FTIR spectra of (a) lyophilized ASF, (b) electrospun ASF/PEO blend, and (c) ASF microparticles.

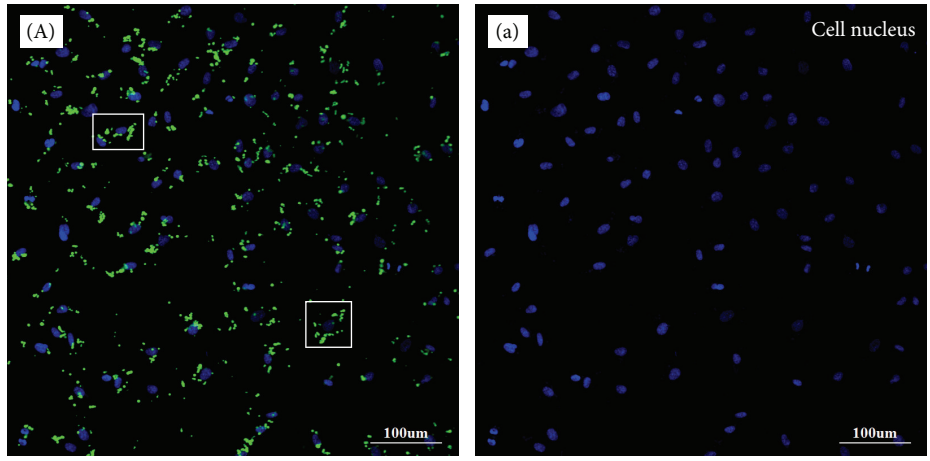

Figure 5: Confocal images of EA926 cells after incubating with ASF microparticles (green) for 2 h. (A) Overlay; (a) cell nucleus (blue).

RGD-integrin interactions. Cellular uptake of fluorescent ASF microparticles was demonstrated by CLSM (Figure 5). After 2 h of incubation with the cells, it was clearly shown that the ASF microparticles are readily adhered to the cells. Once the particles were endocytosed, they were found primarily in the cytoplasm around the nuclear membrane (Figure 5, boxes). The results showed that the ASF microparticles could be effectively transferred into the cells. Therefore, ASF microparticles provide a potentially useful approach to prepare biodegradable and bioactive nanocarriers for drug delivery.

The aqueous-based electrospinning provided a mild method to prepare ASF particles by avoiding using organic solvents. The CCK-8 assay was used to determine cell cytotoxicity (Figure 6). The results indicate that EA926 cells incubated with ASF microparticles with low concentration (100 μg/mL) remained at almost the same viability as the control. The cell viability decreased with the increase in the concentration of ASF microparticles but was still about 80% when the concentration of ASF microparticles was as high as 700 μg/mL. Overall, cell cytotoxicity assays demonstrated that ASF microparticles are relatively nontoxic to EA926 cells. These results provide a simple and green method in the fabrication of ASF microparticles for biomedical applications.

4. Conclusion

Electrospinning particles from *Antheraea pernyi* silk fibroin were studied with a focus on blending with PEO and all

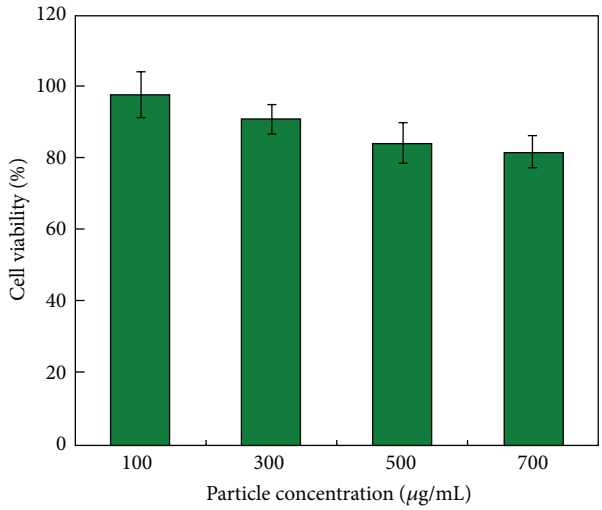

Figure 6: Cytotoxicity profile of ASF microparticles after 24 h incubation with EA926 cells. Percent viability was expressed relative to the control group ($n = 3$).

aqueous processing. To improve the processibility of ASF solutions for electrospinning, biocompatible PEO was successfully blended with the aqueous ASF solution to regulate the formation of bead-on-string structure with well spherical particles. The water-insoluble ASF microparticles with less than 1 μm diameter were obtained after disrupting the nanofibrillar string between particles by aqueous ethanol and ultrasonic treatments. The aqueous-based electrospinning provided a mild method to prepare ASF particles without using organic solvents. The ASF microparticles were relatively nontoxic to EA926 cells and easily uptaken by the cells, providing a potential option for the fabrication of drug carrier.

Competing Interests

The authors declare that there are no competing interests regarding the publication of this paper.

Acknowledgments

This work was supported by the Nature Science Foundation of Wuhan Textile University (155017) and National Nature Science Foundation of China (51303141).

References

[1] A. E. Thurber, F. G. Omenetto, and D. L. Kaplan, "*In vivo* bioresponses to silk proteins," *Biomaterials*, vol. 71, Article ID 17034, pp. 145–157, 2015.

[2] B. Kundu, N. E. Kurland, S. Bano et al., "Silk proteins for biomedical applications: bioengineering perspectives," *Progress in Polymer Science*, vol. 39, no. 2, pp. 251–267, 2014.

[3] Z. Luo, Q. Zhang, M. Shi, Y. Zhang, W. Tao, and M. Li, "Effect of pore size on the biodegradation rate of silk fibroin scaffolds," *Advances in Materials Science and Engineering*, vol. 2015, Article ID 315397, 7 pages, 2015.

[4] A. S. Lammel, X. Hu, S.-H. Park, D. L. Kaplan, and T. R. Scheibel, "Controlling silk fibroin particle features for drug delivery," *Biomaterials*, vol. 31, no. 16, pp. 4583–4591, 2010.

[5] Z. Cao, X. Chen, J. Yao, L. Huang, and Z. Shao, "The preparation of regenerated silk fibroin microspheres," *Soft Matter*, vol. 3, no. 7, pp. 910–915, 2007.

[6] B. Subia, S. Chandra, S. Talukdar, and S. C. Kundu, "Folate conjugated silk fibroin nanocarriers for targeted drug delivery," *Integrative Biology*, vol. 6, no. 2, pp. 203–214, 2014.

[7] P. Shi, S. A. Abbah, K. Saran et al., "Silk fibroin-based complex particles with bioactive encrustation for bone morphogenetic protein 2 delivery," *Biomacromolecules*, vol. 14, no. 12, pp. 4465–4474, 2013.

[8] I. Schultz, F. Vollmers, T. Lühmann et al., "Pulmonary insulin-like growth factor I delivery from trehalose and silk-fibroin microparticles," *ACS Biomaterials Science & Engineering*, vol. 1, no. 2, pp. 119–129, 2015.

[9] J. Wang, S. Zhang, T. Xing et al., "Ion-induced fabrication of silk fibroin nanoparticles from Chinese oak tasar *Antheraea pernyi*," *International Journal of Biological Macromolecules*, vol. 79, pp. 316–325, 2015.

[10] R. You, Y. Xu, Y. Liu, X. Li, and M. Li, "Comparison of the *in vitro* and *in vivo* degradations of silk fibroin scaffolds from mulberry and nonmulberry silkworms," *Biomedical Materials*, vol. 10, no. 1, Article ID 015003, 2015.

[11] X.-Y. Luan, Y. Wang, X. Duan et al., "Attachment and growth of human bone marrow derived mesenchymal stem cells on regenerated antheraea pernyi silk fibroin films," *Biomedical Materials*, vol. 1, no. 4, article 181, 2006.

[12] W. Shao, J. He, F. Sang et al., "Enhanced bone formation in electrospun poly(L-lactic-co-glycolic acid)-tussah silk fibroin ultrafine nanofiber scaffolds incorporated with graphene oxide," *Materials Science and Engineering: C*, vol. 62, pp. 823–834, 2016.

[13] N. Minoura, S.-I. Aiba, M. Higuchi, Y. Gotoh, M. Tsukada, and Y. Imai, "Attachment and growth of fibroblast cells on silk fibroin," *Biochemical and Biophysical Research Communications*, vol. 208, no. 2, pp. 511–516, 1995.

[14] R. Sridhar, R. Lakshminarayanan, K. Madhaiyan, V. A. Barathi, K. H. C. Limh, and S. Ramakrishna, "Electrosprayed nanoparticles and electrospun nanofibers based on natural materials: applications in tissue regeneration, drug delivery and pharmaceuticals," *Chemical Society Reviews*, vol. 44, no. 3, pp. 790–814, 2015.

[15] J. He, Y. Cheng, and S. Cui, "Preparation and characterization of electrospun Antheraea pernyi silk fibroin nanofibers from aqueous solution," *Journal of Applied Polymer Science*, vol. 128, no. 2, pp. 1081–1088, 2013.

[16] H. Cao, X. Chen, L. Huang, and Z. Shao, "Electrospinning of reconstituted silk fiber from aqueous silk fibroin solution," *Materials Science and Engineering C*, vol. 29, no. 7, pp. 2270–2274, 2009.

[17] H.-J. Jin, J. Chen, V. Karageorgiou, G. H. Altman, and D. L. Kaplan, "Human bone marrow stromal cell responses on electrospun silk fibroin mats," *Biomaterials*, vol. 25, no. 6, pp. 1039–1047, 2004.

[18] A. J. Meinel, K. E. Kubow, E. Klotzsch et al., "Optimization strategies for electrospun silk fibroin tissue engineering scaffolds," *Biomaterials*, vol. 30, no. 17, pp. 3058–3067, 2009.

[19] H. Fong, I. Chun, and D. H. Reneker, "Beaded nanofibers formed during electrospinning," *Polymer*, vol. 40, no. 16, pp. 4585–4592, 1999.

[20] K. H. Lee, H. Y. Kim, H. J. Bang, Y. H. Jung, and S. G. Lee, "The change of bead morphology formed on electrospun polystyrene fibers," *Polymer*, vol. 44, no. 14, pp. 4029–4034, 2003.

[21] H.-J. Jin, S. V. Fridrikh, G. C. Rutledge, and D. L. Kaplan, "Electrospinning *Bombyx mori* silk with poly(ethylene oxide)," *Biomacromolecules*, vol. 3, no. 6, pp. 1233–1239, 2002.

[22] M. Li, W. Tao, S. Kuga, and Y. Nishiyama, "Controlling molecular conformation of regenerated wild silk fibroin by aqueous ethanol treatment," *Polymers for Advanced Technologies*, vol. 14, no. 10, pp. 694–698, 2003.

[23] J. Panyam and V. Labhasetwar, "Biodegradable nanoparticles for drug and gene delivery to cells and tissue," *Advanced Drug Delivery Reviews*, vol. 55, no. 3, pp. 329–347, 2003.

[24] Z. Zhen, W. Tang, H. Chen et al., "RGD-modified apoferritin nanoparticles for efficient drug delivery to tumors," *ACS Nano*, vol. 7, no. 6, pp. 4830–4837, 2013.